

GUIDE VANES EMBEDDED VISUALIZATION TECHNIQUE FOR INVESTIGATING FRANCIS RUNNER INTER-BLADE VORTICES AT DEEP PART LOAD OPERATION

Keita YAMAMOTO*

EPFL Laboratory for Hydraulic Machines, Switzerland

Andres MÜLLER

EPFL Laboratory for Hydraulic Machines, Switzerland

Arthur FAVREL

EPFL Laboratory for Hydraulic Machines, Switzerland

Christian LANDRY

EPFL Laboratory for Hydraulic Machines, Switzerland

François AVELLAN

EPFL Laboratory for Hydraulic Machines, Switzerland

ABSTRACT

In hydraulic power plants, it is well known that Francis turbines are subject to various cavitation phenomena under off-design operating conditions, and visualizations have played a key role and performed for understanding and revealing the dynamical behaviour of the cavitation. However, visualizing the cavitation from the high pressure side of the runner has not been successfully carried out yet, due to the complicated structure of a spiral case, stay vanes and guide vanes obstructing the visual access. Therefore, the present study first introduces the visualization technique which enables the optical access to the blade channel through a guide vane, featuring a specially instrumented guide vane with a transparent window, a boroscope with a swivel prism, and a suitable power LED light source. Then, the visualization technique is applied to the case-study of the cavitation vortex developing inside blade to blade channel in the deep part operating condition of a Francis turbine, called inter-blade cavitation vortices. Both the onset and the dynamics of the inter-blade vortices, which have not been fully understood yet, are investigated for the first time using the presented visualization.

KEYWORDS

Francis turbine, deep part load, inter-blade cavitation vortex, visualization technique

* *Corresponding author:* Laboratory for Hydraulic Machines, EPFL, Av. de Cour 33bis, 1007 Lausanne, Switzerland phone: +41 21 69 37382, email: keita.yamamoto@epfl.ch

1. INTRODUCTION

Hydraulic turbines are often subject to the cavitation flow, and various types of cavitation are observed depending on the discharge and head conditions [1, 2]. In particular, the cavitation vortex rope developing in the draft tube cone at the turbine outlet can occasionally generate instabilities and can prevent to operate the generating unit [3]. Therefore, a large number of researches including one-dimensional stability analyses, a hydro-acoustic resonance analysis, and measurements of the velocity field surrounding the cavitation vortex rope have been performed and reported [4, 5, 6, 7]. Recently, in order to compensate for the stochastic nature of variable renewable energy sources, hydraulic turbines are more and more required to enhance their flexibility by extending the operating range down to the deep part load operating condition. However, the characteristics of cavitation phenomena observed in the deep part load operating condition, especially inter-blade cavitation vortices, are not fully understood yet.

For the purpose of understanding and revealing the characteristics and dynamical behaviour of the cavitation, visualizations play a decisive role. Recently, as a first step of the analysis for the inter-blade cavitation vortices, the adapted visualization techniques to properly visualize the inter-blade cavitation vortices from the low pressure side of the turbine through the transparent diffuser cone with an inclined window as shown in Fig. 1 are introduced [8]. However, the visualization of the cavitation from the high pressure side of the turbine has not been successfully conducted yet, due to the complicated structure obstructing the visual access in the high pressure side. Therefore, the present study first introduces the development of the sophisticated visualization technique which enables the optical access to the blade channel through the guide vane, especially featuring the specially instrumented guide vane, a boroscope with a swivel prism covering the variable visual range, and a suitable power LED light source including a brief technical characteristics of the LED lights. Then, this visualization technique is applied for the first time to the case-study of the inter-blade cavitation vortices in the deep part load operating condition using a reduced scale model of a Francis turbine, and both onset and dynamical characteristics of the inter-blade cavitation vortices are investigated.



Fig. 1 Experimental setup for high speed visualization of inter-blade cavitation vortices

2. VISUALIZATION TECHNIQUE

A special guide vane equipped with a transparent acrylic glass window and its dimensions are shown in Fig. 2. The hollow guide vane is manufactured, and the transparent window which has a 2 mm thickness and the same surface profile as an original guide vane is attached. The

window is perfectly sealed by an epoxy resin in order to isolate the embedded equipment from the pressurised water in the spiral case. The dimension of the instrumented guide vane is made completely same as the original one, and the surface of the guide vane and window is sufficiently polished and made smooth in order not to influence the flow and efficiency of the turbine.

For the optical access to the blade channel through the instrumented guide vane, a boroscope is adopted. Generally, a boroscope is used for enabling a visual access to an inaccessible area by a deflecting prism as shown in Fig. 3. The selected boroscope for the present application (8.10026.093, R. WOLF) features a swivel deflecting prism covering a various direction of view including the visual range from the hub to shroud, which can be especially used for investigating the onset of the inter-blade cavitation vortices. The boroscope has a design (ϕ 10 mm and 260 mm working length) fitting perfectly into the guide vane hollow (see Fig. 4). The boroscope can be rotated as shown by the arrow in Fig. 4, enabling to change the field of view to visualize different parts of the blade including the pressure and suction sides.

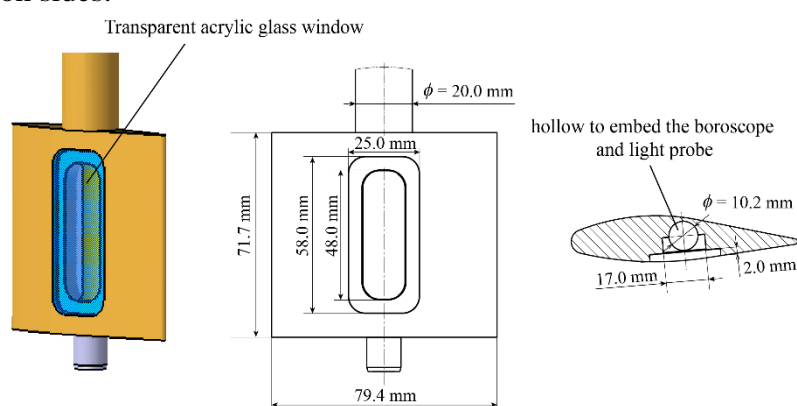


Fig. 2 Sketch of the hollow guide vane equipped with a transparent acrylic glass window

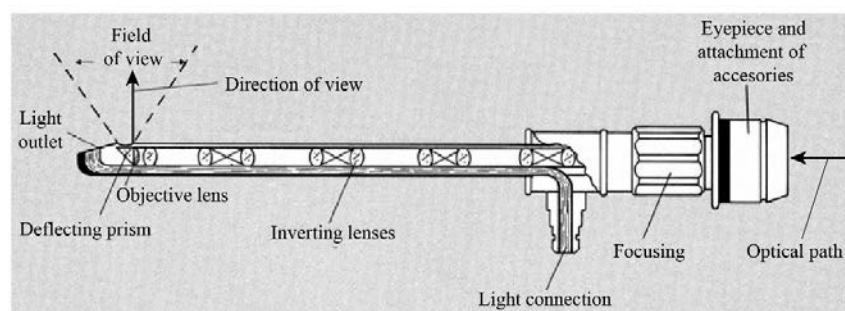


Fig. 3 General structure of the boroscope

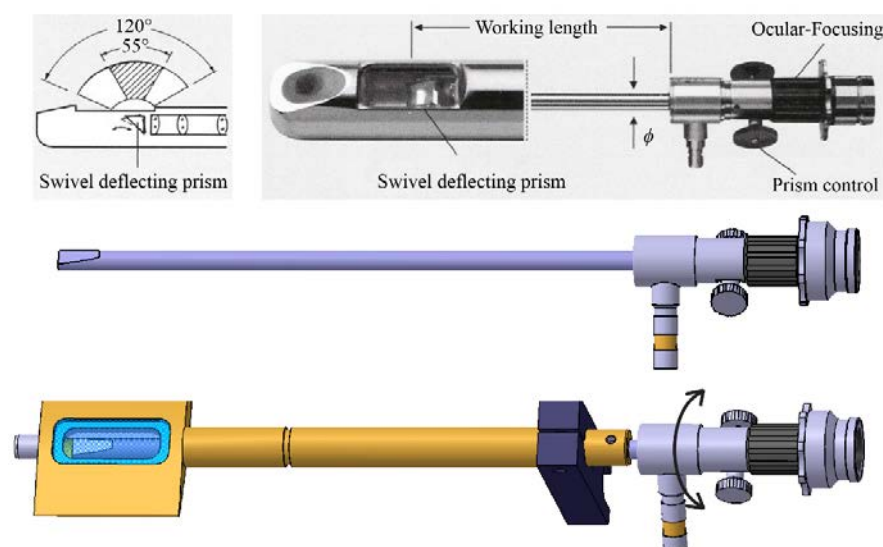


Fig. 4 Selected boroscope featuring a swivel deflecting prism

As a light source, a compact power LED (XP-L V5, CREE) with a dimension $3.45 \text{ mm} \times 3.45 \text{ mm}$ as shown in Fig. 5 is installed. The type of the LED is carefully selected, particularly considering the luminous flux, thermal efficiency, and wavelength of light [11] to improve the penetration of light in water. About 6000 K of the Correlated Colour Temperature range, CCT range, where the light has the most effective wavelength for the penetration of light in water [11] is selected for the LED, taking into account the least loss of the light reaching the blade channel. The used LED features a maximum power 10 W and a maximum luminous flux 1058 lm at 3 A current, and its electric characteristics and luminous flux with respect to the forward current provided by the manufacturer are shown in Fig. 6. The LED is driven at the maximum current and luminous flux highlighted by the green mark in Fig. 6. The LED is attached to an effective aluminium heat sink to improve the radiation performance and reduce the risk of damage to the acrylic glass window, then, the 5 sets of the LEDs are installed on the special probe which has the same diameter and working length as the boroscope for the versatile use (see Fig. 7). The probe can be rotated in a same way of the boroscope, and the inside of the blade channel is properly illuminated by optimizing the rotation angle of the probe. Totally 10 LED lights with two probes are prepared, and each 5 sets of the LEDs with a proper resistance of 1Ω are connected in series to the LED controller (RT-420-20, GARDASOFT) generating a pulsed electric current. The pulse width of the current is set to 0.2 ms to adjust a sharpness of the image.

Finally, the image is acquired by a medium frame rate camera (DFK23G445, IMAGINGSOURCE) connected to the boroscope. The connection system as well as the electric schematic are shown in Fig. 8. Both frequencies of the pulsed current and the image acquisition of the camera are synchronized with the rotational frequency of the turbine as shown in Fig. 8, in order to acquire an image at the same timing of the LED light emission. The entire installation of the instrumented guide vane, boroscope and the probe with the LED lights is shown in Fig. 9.

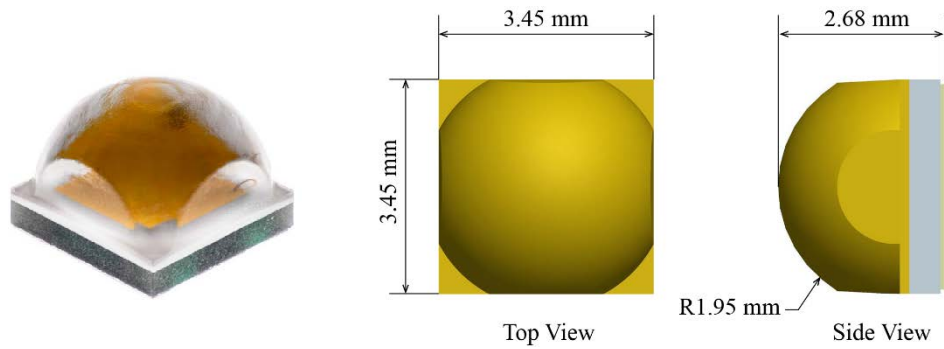


Fig. 5 Compact power LED and its dimension

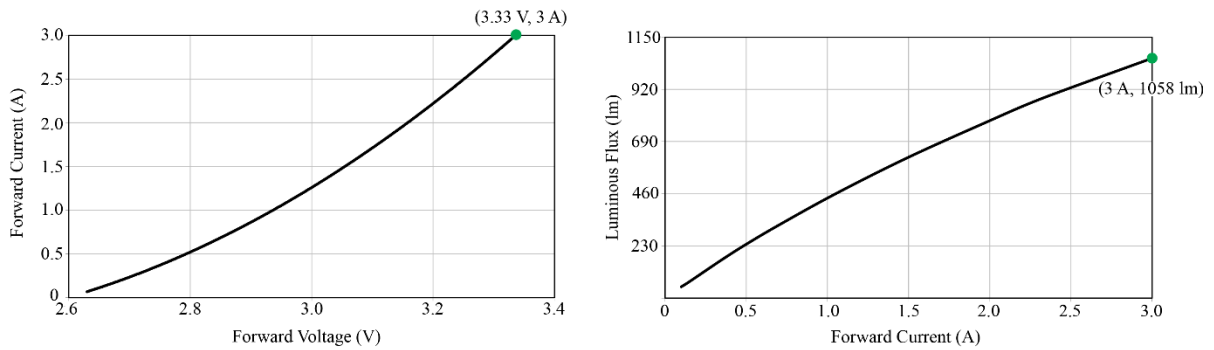


Fig. 6 Electrical characteristics and luminous flux with respect to a forward current of the LED

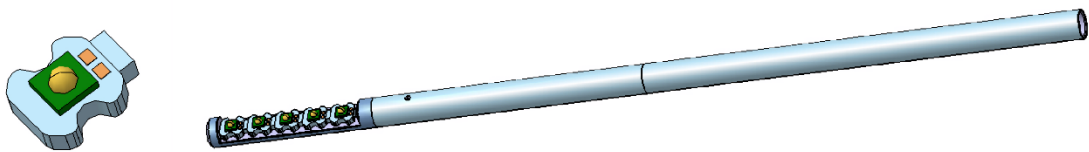


Fig. 7 LED light attached to an aluminium heat sink and the probe for LED lights

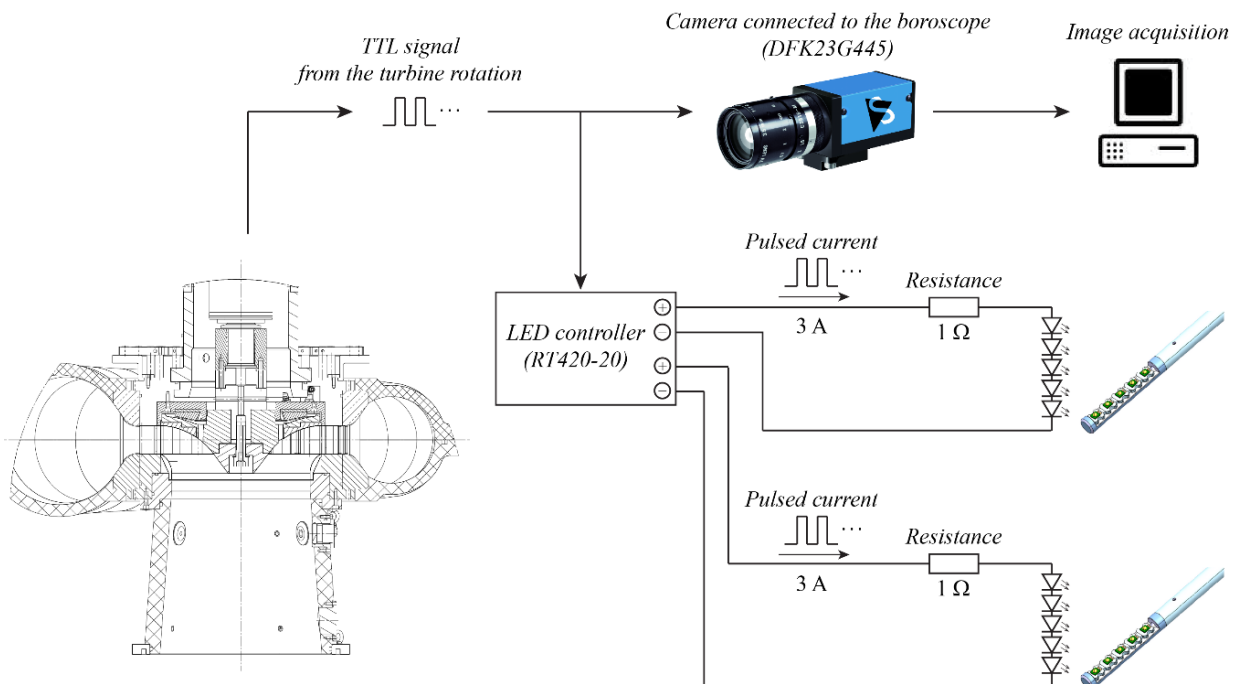


Fig. 8 Sketch of the connection for the acquisition system and LED

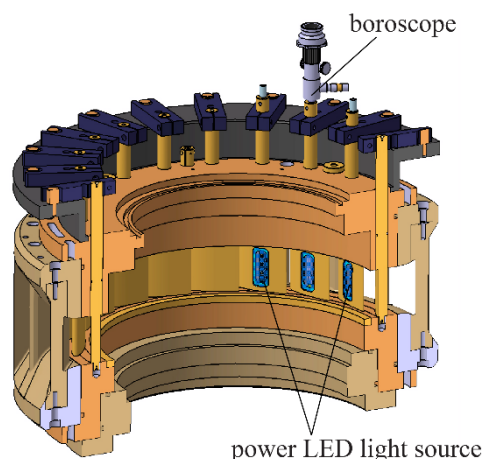


Fig. 9 Entire installation of the instrumented guide vane, boroscope, and LED light source

3. EXPERIMENTAL FACILITY

The experiments are carried out with a 1:16 reduced scale model of a Francis turbine which has a specific speed $\nu = 0.27$. There are 8 piezo-resistive pressure sensors installed in the draft tube cone at the runner outlet and 4 sensors in the guide vane in order to monitor the characteristics of the cavitation phenomena. The torque acting on the shaft, mean discharge, turbine rotational frequency, and turbine specific energy are also monitored and recorded throughout all the measurements. The mean discharge is adjusted by the guide vane opening angle, and the turbine specific energy is controlled by the rotational frequency of two axial double-volute pumps. The pressure level in the draft tube is set by a vacuum pump in the downstream reservoir.

In the present study, the experiments are carried out focusing on two different turbine head conditions at a fixed guide vane opening angle ($\alpha = 5$ degree), which are summarized in the following table. In addition to the visualization through the instrumented guide vane, the visualization from the low pressure side of the runner which is already described in [8] is also carried out.

OP	GV. Opening α	Rotating frequency n	Specific energy E	Q/Q_{BEP}	σ
DPL1	5	13.33 Hz	263 J kg ⁻¹	26.3 %	0.11
DPL2	5	14.67 Hz	263 J kg ⁻¹	27.0 %	0.11

Tab.1 Operating conditions for the measurements

4. RESULTS

The comparison of the visualization results acquired by the different field of view by optimizing the angle of the swivel prism and the boroscope rotation as mentioned above, as well as the visualization from the low pressure side of the turbine for the two different operating conditions is shown in Fig. 10. It can be observed that the inter-blade cavitation vortices are not seen in DPL1, on the other hand, the cavitation is clearly developed with its shape twisted inside the blade channel in the case of DPL2. The visualization through the guide vane demonstrates that the inter-blade cavitation vortex is attached on the hub, and the cavitation is formed toward the blade trailing edge. All the visualization results evidence that the inter-blade cavitation vortex is successfully captured by using the presented visualization.

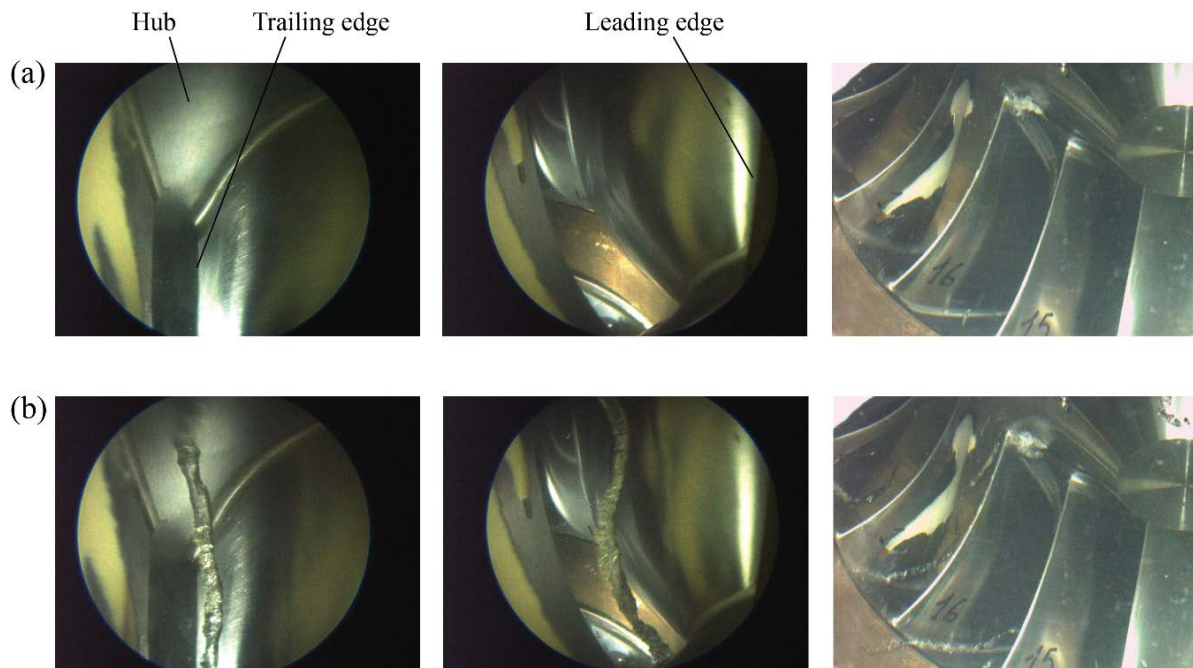


Fig. 10 Visualization results of two different operating conditions, DPL1 (a) and DPL2 (b)

5. CONCLUSION

This paper presents the visualization technique featuring the instrumented guide vane with the transparent acrylic glass window, the boroscope with the swivel deflecting prism, and the suitable power LED light source. It is shown that the inter-blade cavitation vortex is successfully captured by the introduced visualization, and it is confirmed that the inter-blade cavitation vortex is attached on the hub, and then formed toward the trailing edge. This successful evaluation of the inter-blade cavitation vortex by the visualization enables further investigations to accurately survey its mechanism and dynamical characteristics.

6. ACKNOWLEDGEMENTS

The research leading to the results published in this paper is part of the HYPERBOLE research project, granted by the European Commission (ERC/FP7- ENERGY-2013-1-Grant 608532). The authors would also like to thank BC Hydro for making available the reduced scale model, in particular Danny Burggraeve and Jacob Iosfin. Moreover, the authors would like to acknowledge the commitment of the Laboratory for Hydraulic Machines' technical staff, especially Georges Crittin, Maxime Raton, Alain Renaud, Philippe Faucherre and Vincent Berruex.

7. REFERENCES

- [1] Avellan, F. (2004). Introduction to Cavitation in Hydraulic Machinery, Proc. of the *6th International Conference on Hydraulic Machinery and Hydrodynamics*, Timisoara, Romania

- [2] Escaler, X., Egusquiza E., Farhat, M., Avellan, F. and Coussirat, M. (2006). Detection of cavitation in hydraulic turbines, *Journal of Mechanical Systems and Signal Processing*, Vol.20, Issue4, pp.983-1007
- [3] Rheingans, W. J. (1940). Power Swings in Hydroelectric Power Plants, *Transaction of ASME* 62, pp.171-184
- [4] Alligné, S., Nicolet, C., Tsujimoto, Y., & Avellan, F. (2014). Cavitation surge modelling in Francis turbine draft tube. *Journal of Hydraulic Research*, 52, 399–411
- [5] Müller, A., Bullani, A., Dreyer, M., Roth, S., Favrel, A., Landry, C. and Avellan, F. (2012) Interaction of a pulsating vortex rope with the local velocity field in a Francis turbine draft tube. *IOP Conference Series: Earth and Environmental Science*, vol 15, pp.032-038
- [6] Müller, A., Dreyer, M., Andreini, N., Avellan, F. (2013). Draft tube discharge fluctuation during self-sustained pressure surge: Fluorescent particle image velocimetry in two-phase flow, *Experiments in Fluids*, Vol.54, Issue 4, pp.1-11
- [7] Favrel A., Landry C., Müller A. and Avellan F. (2012). Experimental identification and study of hydraulic resonance test rig with Francis turbine operating at partial load, *Proc. of the 26th IAHR Symposium on Hydraulic Machinery and Systems* Beijing, China
- [8] Yamamoto K., Müller A., Favrel A., Landry C., Avellan F. (2014). Pressure measurements and high speed visualizations of the cavitation phenomena at deep part load condition in a Francis turbine, *Proc. of the 27th IAHR Symposium on Hydraulic Machinery and Systems* Montreal, Canada
- [9] Marvin R. Querry, David M. Wieliczka, David J. Segelstein. (1997). Water (H₂O). *Handbook of Optical Constants of Solids*, pp.1059-1077.

8. NOMENCLATURE

E	(J kg ⁻¹)	specific energy
n	(Hz)	rotating frequency
Q	(m ³ s ⁻¹)	discharge
σ	(-)	Cavitation number